On-chip temperature-compensated Love mode surface acoustic wave device for gravimetric sensing

Q. Liu[a) and A. J. Flewitt

Electrical Engineering Division, Department of Engineering, University of Cambridge, 9 JJ

Thomson Ave, CB3 0FA, United Kingdom

ABSTRACT

Love mode surface acoustic wave (SAW) sensors have been recognized as one of the most sensitive devices for gravimetric sensors in liquid environments such as bio sensors. Device operation is based upon measuring changes in the transmitted (S_{21}) frequency and phase of the first-order Love wave resonance associated with the device upon on attachment of mass. However, temperature variations also cause a change in the first order S_{21} parameters. In this work, shallow grooved reflectors and a 'dotted' single phase unidirectional interdigitated transducer (D-SPUDT) have been added to the basic SAW structure which promote unidirectional Love wave propagation from the device's input interdigitated transducers. Not only does this enhance the first-order S_{21} signal, but it also allows propagation of a third-order Love wave. The attenuation coefficient of the third-order wave is sufficiently great that, whilst there is a clear reflected S_{11} signal, the third-order wave does not propagate into the gravimetric sensing area of the device. As a result, whilst the third-order S_{11} signal is affected by temperature changes, it is unaffected by mass attachment in the sensing area. It is shown that this signal can be used to remove temperature effects from the first-order S_{21} signal in real time. This allows gravimetric

---

[a) Author to whom correspondence should be addressed. Electronic address: ql238@cam.ac.uk.

sensing to take place in an environment without the need for any other temperature measurement or temperature control; this is a particular requirement of gravimetric biosensors.

Surface acoustic wave (SAW) devices have received significant interested for biosensing applications due to their small size, low cost of production and low power consumption.[1] Among all the SAW sensors, Love mode acoustic wave sensors have been proved to be one of the most sensitive and reliable biosensors as there is very little acoustic wave energy attenuation through losses into the liquid environment.[2] To generate high quality Love wave resonance, a piezoelectric substrate with a high electromechanical coupling coefficient needs to be used. However, high coupling coefficient materials normally also have high temperature coefficient of frequency,[3] which will cause similar changes to the resonance when the temperature varies as when mass loading occurs, leading to an ambiguous result. There have been several attempts to mitigate this phenomenon. One approach is based on a dual-channel delay line configuration.[4] For example, in a biological measurement, one channel is used for the biological sample itself, and another to provide a temperature reference, allowing the temperature effect to be compensated by subtracting the reference channel signal from the sample signal.[5] However, the two channels configuration leads to increased cost and complexity as two channels are required for RF measurement. Moreover, there is significant cross-talk between the two channels on chip leading to noise.[6] Another method for temperature compensation is to produce a layered structure of piezoelectric materials with opposite temperature coefficients,[7] but there is very limited choice for negative temperature coefficient materials.[8] TeO_2 is one such material,[9] but the additional requirement that it must act as a Love wave

guide layer at the same time means that its use is rarely successful. On the device packaging level, an alternative approach is to embed a thermistor in to the microfluidic chamber to measure the temperature variation and feed this back to a ceramic heater to control the device temperature,[10] but this method is complicated to fabricate and is still very difficult to guarantee a stable chamber temperature due to control difficulties.

In this paper, a method of separating temperature effects from mass loading effects is presented. This utilizes the third-order Love wave resonance reflection S_{11} as a reference signal which is optimized to be sensitive to temperature changes, but is unaffected by mass loading of in the gravimetric sensing area. The energy in higher order resonances is easily dissipated by reflections from the interdigitated transducer (IDT) structure or is overwhelmed by noise. Therefore, in this work, the sensor is purposely optimized to obtain a high quality third-order Love wave resonance by using a 'dotted' single-phase unidirectional transducer (D-SPUDT),[11] and shallow grooves in a ZnO layer on $LiNbO_3$ Love wave device, as show in the device schematic in Fig. 1.

The sensor is based on 64^0 Y-X cut Lithium niobate substrate which offers a high piezoelectric coupling coefficient for generating a shear horizontal wave.[12] After substrate cleaning, AZ5214E photoresist is patterned to define the D-SPUDT structure, 150 nm thick alumium is thermally evaporated on top and the structure formed by lift off. This D-SPUDT is specially designed to minimize both the acoustic energy loss and IDT reflection noise, as highlighted by top right image in Fig.1. The interleaved fingers of the D-SPUDT have width of 1/8 λ_0 and 3/8 λ_0 respectively,

where λ_0 is the wavelength of resonant Love mode SAW. Dot elements have been distributed on the wider fingers of the D-SPUDT with a ratio of 1:1. These features can efficiently inhibit the inter-finger reflection noise and electrical regeneration reflection noise.[13] Following D-SPUDT fabrication, the ZnO Love wave guiding layer was deposited by a HiTUS (High Target Utilization Sputtering) system which offers high uniformity, low stress and highly oriented ZnO films.[14] Finally shallow grooves in the ZnO guiding layer are etched by 0.11% hydrochloric acid to enhance the Love wave resonance, as shown in the top left image in Fig.1. The IDTs are wire-bonded to SMA connectors and the whole device is securely mounted on a high purity copper plate to minimize capacitively-coupled RF noise, as shown in the top middle image in Fig. 1.

Real-time temperature compensation was achieved by LabVIEW software control of an Agilent E5062A network analyzer. As outlined by the measurement flow chart shown in Fig. 1, a frequency sweep is controlled by the LabVIEW program to distinguish the first-order Love wave S_{21} peak and the third-order Love wave S_{11} peak from the Rayleigh wave resonant peaks and other noise signals. Once the relevant resonant peaks have preen identified, to achieve a real time compensation, LabVIEW controls a quick phase measurement of the first-order S_{21} resonance and third-order S_{11} resonance. By applying temperature calibration, weighting for the phase changes of the first-order S_{21} and third-order S_{11} signals are obtained; the two weighted signals are subtracted to extract the mass loading effect from any temperature-dependent effect.

Due to the fact that a high quality third-order resonant peak is difficult to obtain but is critical for the generation of a temperature reference signal, specially designed shallow groove reflectors and D-SPUDTs have been used to enhance the third-order resonance. Fig. 2(a) shows the S_{11} signal for a simple IDT (without any reflectors or D-SPUDTs); it only shows the noticeable first-order resonance peak. As the Love wave propagates mainly in the top section of the guiding layer,[15] the shallow etched grooves are added to specifically enhance the Love wave resonance rather than Rayleigh wave. A grooved device (Fig. 2(b)) shows a higher first-order resonance peak than the simple IDT device in Fig. 2(a), but due to strong IDT reflection leading to energy dissipation and triple transit signal noise,[16] the third-order resonance peak is still not noticeable. By applying D-SPUDTs, more Love wave energy propagates towards the output IDTs, and the IDT reflection and triple transit noise reduces; this yields a clear third-order resonant peak as shown in Fig. 2(c). By adding shallow grooves on the D-SPUDT devices, the third-order resonant peak is further enhanced, as shown in Fig. 2(d). In addition, the quality factor of the grooved D-SPUDT sensor third-order resonance has been enhanced to 186 comparing with a Q factor of 149 in non-grooved D-SPUDT sensors in Fig. 2(c).

Having achieved a high Q third-order resonance using the grooved D-SPUDT device, the temperature response was studied. As shown in Fig. 3, the first-order resonance shows a linear phase change as a function of temperature in the measured range of 15 °C to 62.5 °C, whilst the third-order resonance phase change shows a good fit to a second-order polynomial. It is the fitting to these two curves that allows weighting of the signals when subtracting one from the other to determine the effect of mass loading alone. The third-order phase change reached a maximum point at 52 °C. This

determines the upper limit of temperature compensation for this device, which is sifficiently high for many sensing applications; it is likely that this range could be extended by further optimisation of the device design.

The third-order resonance must be insensitive to the liquid mass load changes in order to act as a temperature reference signal in real sensing environments. Fig.4 (a) shows the third-order phase change when a 20 μl water droplet is placed on or close to the IDTs as a function of distance (0 is when the edge of the drop is just touching the input IDTs, positive distances represent a gap between the drop edge and the IDT, and negative distances represent an overlap of the drop and IDT). The temperature was held constant. The third-order phase is only affected when the drop is on or within ~200 μm of the IDT. Therefore, the third-order resonance phase is insensitive to mass loading in the gravimetric sensing area, as the higher frequency results in strong energy dissipation with distance away from the IDT.

The second-order resonance has also been considered as a possibility for temperature referencing in a similar way to the third-order resonance. Fig.4.(b) shows the phase change comparison between the second-order and third-order resonance, for a 500 μm distance between the water drop and the input IDT. Whilst the third-order resonance is insensitive to the water drop, the second-order resonance shows a clear phase change; this is still the case when the water drop is moved to be 3 mm away from the edge of input IDTs, which means that the second-order resonance is not suitable for a temperature reference. The reason for this difference between the second- and third-order response is understood by considering the transmission coefficient S_{21} in Fig. 4(c). There is clear second-order S_{21} resonant peak but no third-order S_{21} resonant

peak. This means the third-order Love wave cannot propagate to the output IDTs while the second order Love wave still can propagate to the output IDTs, meaning that the second-order Love wave is strongly affected by mass loading in the gravimetric sensing area.

Having demonstrated that the third-order Love wave is insensitive to mass loading in the sensing area, real time temperature compensation has been carried out using LabVIEW. As shown in Fig. 5, a 20 μl water drop is attached and removed from the central sensing area over a period of ~250 s. In addition, a hot plate was used to increase the temperature of the device from ambient to 45 °C for ~50 s during this period before being allowed to cool again. The as-measured first-order S_{21} signal (dashed red line) is affected by both liquid and temperature, whereas the third-order S_{11} signal (solid blue) is only affected by temperature. Therefore, by measuring the device first so that the quantitative effect of temperature change alone upon both the first-order S_{21} and third-order S_{11} is known, it is possible to determine a calibration factor that links the two. Therefore, when the device is subjected to both mass and temperature changes, the effect of the temperature change on the S_{21} signal can be subtracted using the S_{11} signal, thereby allowing the mass change to be determined from the residual S21 signal.

In summary, a method for correcting for temperature changes in gravimetric surface acoustic wave sensors is presented. A first-order Love wave provides the main measurement signal for mass changes and a third-order Love wave allows temperature correction. The third-order Love wave is enhanced by use of both shallow groove reflectors and dotted Single Phase Unidirectional Transducers (D-

SPUDTs), resulting in a resonant Q factor of 186. The third-order resonance shows broad temperature from 15 °C to 52 °C. The third-order Love wave is insensitive to mass changes in the sensing area due to its high attenuation (this is not the case for the second-order Love wave). Real time temperature compensation is demonstrated by subtracting the amplified third-order phase change from the first-order phase change using LabVIEW. Such a device is particularly suited to bio sensing applications.

1.   M. Hoummady, A. Campitelli and W. Wlodarski, Smart Materials and Structures **6** (6), 647 (1997).

2.   G. Kovacs and A. Venema, Appl. Phys. Lett. **61** (6), 639-641 (1992).

3.   K. Hashimoto, *Surface Acoustic Wave Devices in Telecommunications Modelling and Simulation*. (Springer, 2000).

4.   E. N. M.J. Vellekoop, J.C. Haartsen and A. Venema,, IEEE 1987 Ultrasonics Symposium (unpublished).

5.   S. Li, Y. Su, Y. Wan and Z. Tang, in *International Conference on Sensing Technology* (IEEE, Wellington, 2013), pp. 62-66.

6.   Y.-T. Shen, C.-L. Huang, R. Chen and L. Wu, Sensors and Actuators B: Chemical **107** (1), 283-290 (2005).

7.   C. J. Zhou, Y. Yang, H. L. Cai, T. L. Ren, M. S. Chan and C. Y. Yang, Ieee Electron Device Letters **34** (12), 1572-1574 (2013).

8.   D. B. Armstrong, Patent No. US3894286 A (8th Jul, 1975).

9.   N. Dewan, S. P. Singh, K. Sreenivas and V. Gupta, Sensors and Actuators B: Chemical **124** (2), 329-335 (2007).

10.   H. Tarbague, J.-L. Lachaud, S. Destor, L. Velutini, J.-P. Pillot, B. Bennetau, D. Moynet, D. Rebière, J. Pistre and C. Dejous, ECS Transactions **23** (1), 319-325 (2009).

11.   T. Kodama, H. Kawabata, Y. Yasuhara and H. Sato, Ieee Transactions on Ultrasonics Ferroelectrics and Frequency Control **34** (3), 405-405 (1987).

12.   A. Safari and E. Koray Akdogan, *Piezoelectric and Acoustic Materials for Transducer Applications*. (Springer, 2010).

13.   E. M. Garber, D. S. Yip and D. K. Henderson, Ieee Ultrasonics Symposium Proceedings **1** (3), 7-12 (1994).

14.   L. Garcia-Gancedo, J. Pedros, Z. Zhu, A. J. Flewitt, W. I. Milne, J. K. Luo and C. J. B. Ford, Journal of Applied Physics **112** (1), 7 (2012).

15.   P. Tournois and C. Lardat, IEEE Trans. Sonics Ultrasonics **16** (3), 107-116 (1969).

16.   D. P. Morgan, *Surface acoustic wave filters : with applications to electronic communications and signal processing*, 2nd ed. (Academic Press, Oxford, UK, 2007).
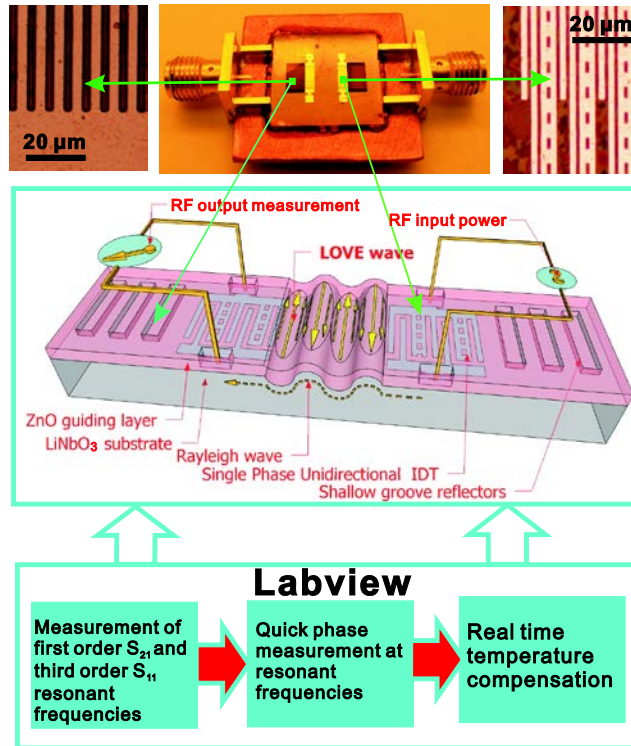
Fig. 1. Top: photograph of the packaged sensor device with high resolution images of the grooved reflectors (left) and D-SPUDTs (right). Middle: schematic diagram of the SAW sensor device. Bottom: flow diagram of the mode of operation.
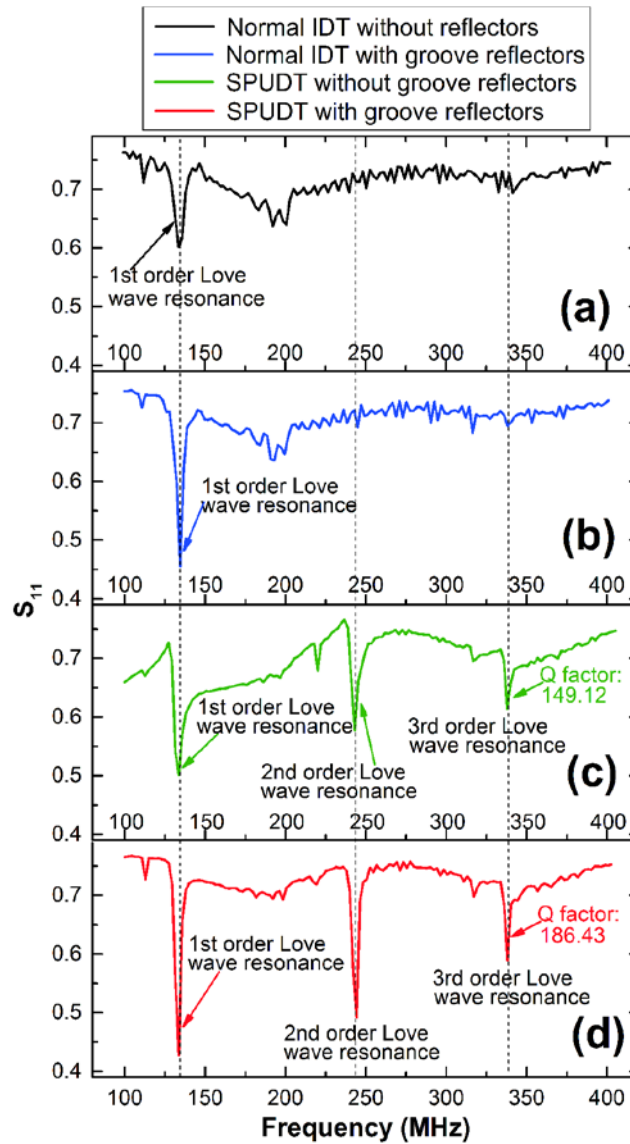
Fig. 2. (a) Resonant peaks for a simple IDT device without grooved reflectors or D-SPUDTs. (b) Resonant peaks for an IDT sensor with grooved reflectors. (c) Resonant peaks for a device with D-SPUDTs but without grooved-reflectors. (d) Resonant peaks for a device with D-SPUDTs and grooved-reflectors. The shallow groove reflectors and D-SPUDTs show clear enhancement of the third-order signal.
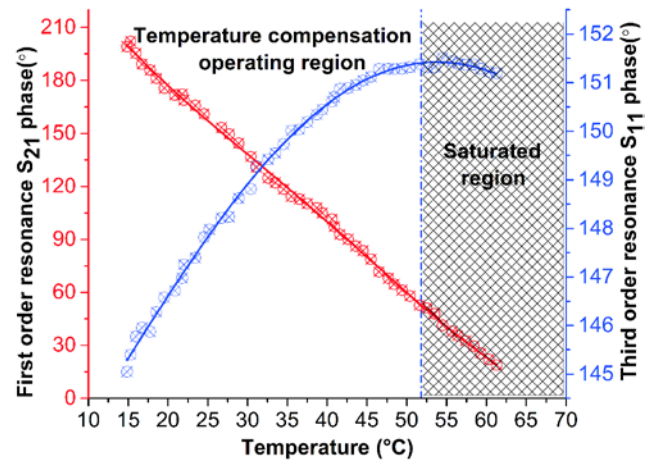
Fig. 3. Variations in the phase of the first-order Love wave S_{21} coefficient and third-order S_{11} coefficient.
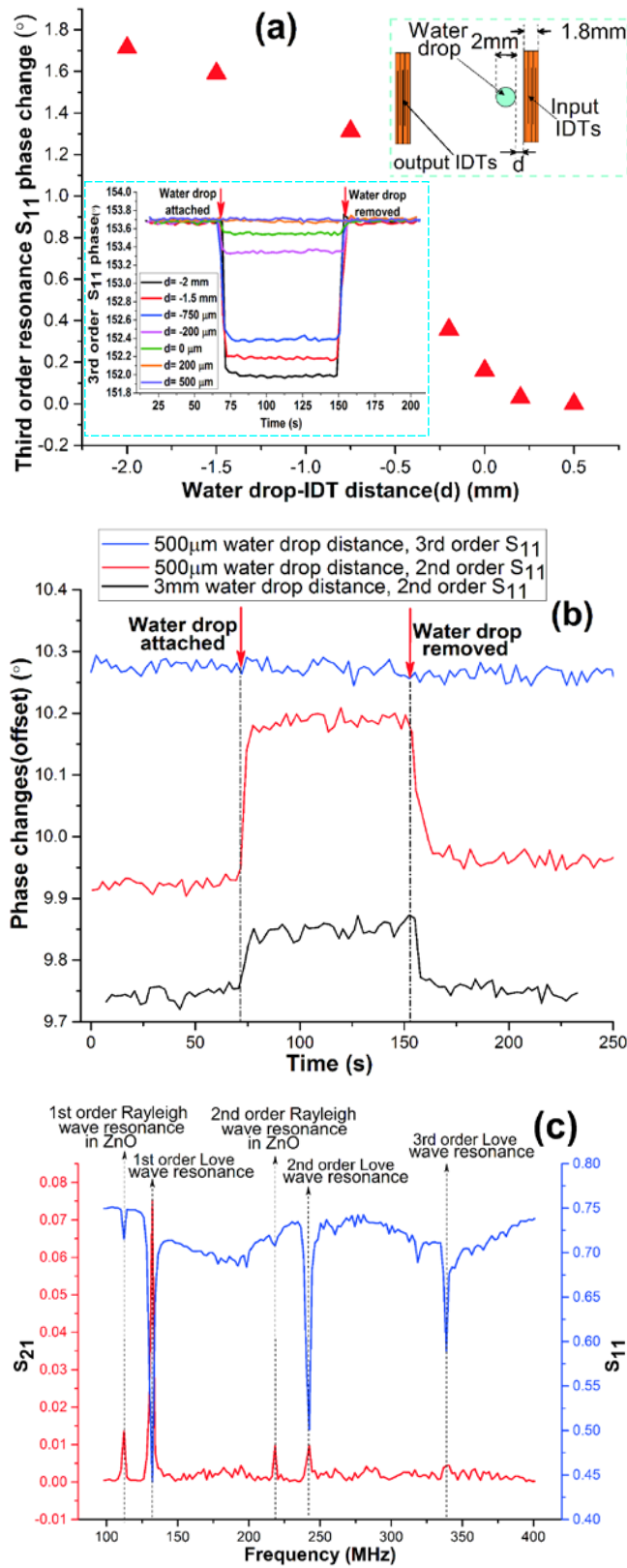
Fig. 4. (a) Third-order phase change when a 20 μl water droplet is placed on or close

to the IDTs as a function of distance (0 is when the edge of the drop is just touching

the input IDTs, positive distances represent a gap between the drop edge and the IDT

and negative distances represent an overlap of the drop and IDT). (b) Comparison of the second-order phase change and third-order phase change for different water drop distances. The second-order signal shows much greater sensitivity to mass loading in the gravimetric sensing area. (c) Comparison of S_{11} and S_{21} signals indicating that the third-order Love wave is confined close to the input IDT, whereas the second-order Love wave noticeably propagates through the gravimetric sensing area to the output IDT.
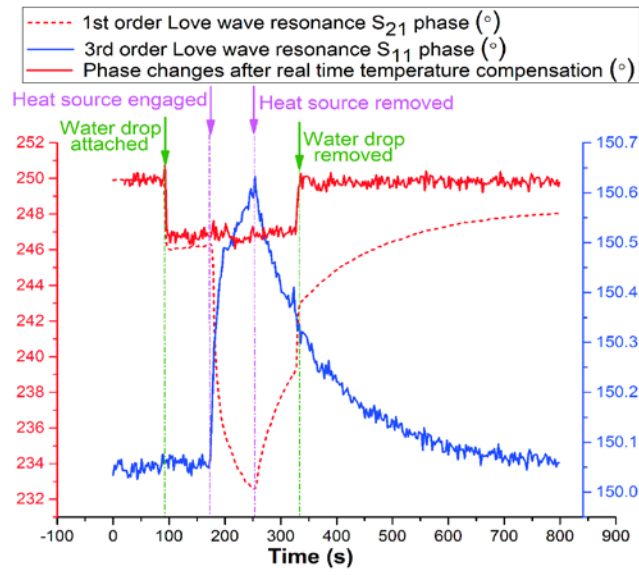
Fig. 5. Real time temperature compensation (in solid red) using the first-order phase signal (in dashed red) corrected for temperature changes by the third-order phase (in solid blue).